

AD-A045 997

EMMANUEL COLL BOSTON MASS
CALIBRATION OF THE SSJ/3 SENSOR ON THE DMSP SATELLITES. (U)

F/G 14/2

SEP 77 A HUBER, J PANTAZIS, A L BESSE

F19628-76-C-0039

SCIENTIFIC-2

AFGL-TR-77-0202

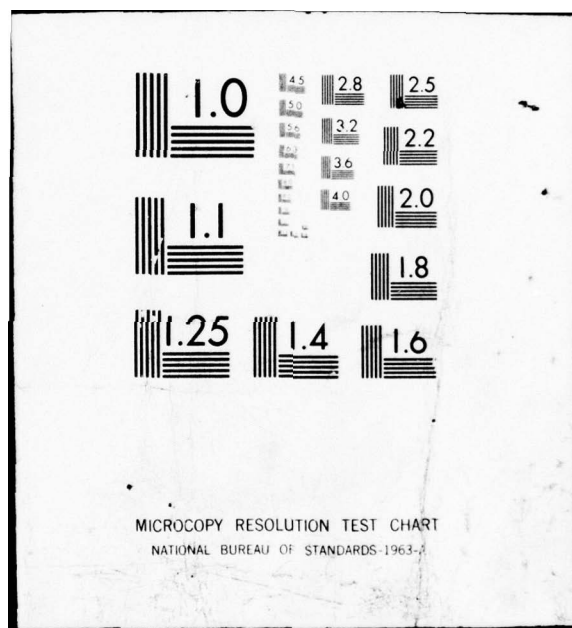
NL

UNCLASSIFIED

| OF |
AD.
A045 997



END
DATE
FILED
11-77
DDC



MICROCOPY RESOLUTION TEST CHART
NATIONAL BUREAU OF STANDARDS-1963-A

AD A 045997

(12)

AFGL-TR-77-0202

CALIBRATION OF THE SSJ/3 SENSOR ON THE DMSP SATELLITES

ALAN HUBER
JOHN PANTAZIS
A.L. BESSIE
P.L. ROTHWELL

THE TRUSTEES OF EMMANUEL COLLEGE ✓
400 THE FENWAY
BOSTON MASSACHUSETTS 02115

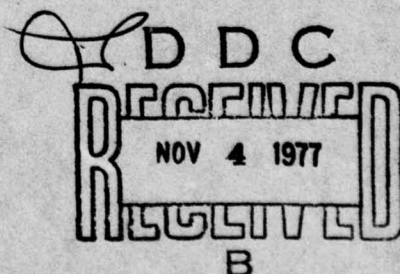
SEPTEMBER 1977

SCIENTIFIC REPORT NO. 2 ✓

APPROVED FOR PUBLIC RELEASE; DISTRIBUTION UNLIMITED

AIR FORCE GEOPHYSICS LABORATORY
AIR FORCE SYSTEMS COMMAND
UNITED STATES AIR FORCE
HANSOM AFB, MASSACHUSETTS 01731

AD No. _____
DDC FILE COPY



Qualified requestors may obtain additional copies from the Defense Documentation Center. All others should apply to the National Technical Information Service.

UNCLASSIFIED

MIL-STD-847A
31 January 1973

SECURITY CLASSIFICATION OF THIS PAGE (When Data Entered)

REPORT DOCUMENTATION PAGE			READ INSTRUCTIONS BEFORE COMPLETING FORM
1. REPORT NUMBER AFGL-TR-77-0202	2. GOVT ACCESSION NO.	3. RECIPIENT'S CATALOG NUMBER	
4. TITLE (AND SUBTITLE) CALIBRATION OF THE SSJ/3 SENSOR ON THE DMSP SATELLITES.		5. TYPE OF REPORT AND SCOPE COVERED SCIENTIFIC 20-2 01APR77 - 01SEP77	
7. AUTHOR ALAN HUBER* JOHN PANTAZIS		6. PERFORMING ORG. REPORT NUMBER F19628-76-C-0039	
8. CONTRACT OR GRANT NUMBER(S) 10		10. PROGRAM ELEMENT, PROJECT, TASK AREA & WORK UNIT NUMBER 61102F 2311G102	
9. PERFORMING ORGANIZATION NAME AND ADDRESS EMMANUEL COLLEGE 400 THE FENWAY BOSTON MA 02115		11. REPORT DATE SEPTEMBER 1977	
12. CONTROLLING OFFICE NAME AND ADDRESS AIR FORCE GEOPHYSICS LABORATORY HANSOM AFB MA 01731 CONTRACT MONITOR: ROBERT C. FILZ (PHG)		13. NUMBER OF PAGES 42	
14. MONITORING AGENCY NAME & ADDRESS (if different from Controlling Office) Rept. for 1 Apr - 1 Sep 77		15. SECURITY CLASS. (of this report) UNCLASSIFIED	
16. DISTRIBUTION STATEMENT (of this Report) A - APPROVED FOR PUBLIC RELEASE; DISTRIBUTION UNLIMITED 1243p6		15a. DECLASSIFICATION DOWNGRADING SCHEDULE	
17. DISTRIBUTION STATEMENT (of the abstract entered in Block 20, if different from Report) D D C RECORDED NOV 4 1977 B			
18. SUPPLEMENTARY NOTES *PHYSICS RESEARCH DIVISION, EMMANUEL COLLEGE			
19. KEY WORDS (Continue on reverse side if necessary and identify by block number) SSJ/3 SENSOR CHANNELTRON MONTE CARLO CODE ELECTROSTATIC ANALYZER			
20. ABSTRACT (Continue on reverse side if necessary and identify by block number) The SSJ/3 sensor is designed to measure electrons from 50 eV to 20 keV. This is accomplished by using two head assemblies with common signal processing and voltage sources. The low-energy head assembly selects 50.0 to 1,000 eV electrons over eight channels with a normalization factor $H = 4.3 \times 10^{-5} \text{ cm}^2/\text{ster}$. The high-energy assembly similarly selects 1.00 to			

DD FORM 1 JAN 73 EDITION OF 1 NOV 55 IS OBSOLETE

UNCLASSIFIED

SECURITY CLASSIFICATION OF THIS PAGE (When Data Entered)

128 950

LB

MIL-STD-847A
31 January 1973

UNCLASSIFIED

0.000013 SQ CM-STER.

SECURITY CLASSIFICATION OF THIS PAGE (When Data Entered)

20.0 keV electrons over eight channels with an H-factor equal to $1.30 \times 10^{-5} \text{ cm}^2\text{-ster}$.

Energy resolution is approximately 10% for an isotropic incident flux. An electron beam was used to determine angular and energy response. These measurements were compared with results from a Monte-Carlo computer code and approximate analytic methods to determine the final normalizations.

ACCESSION for		
NTIS	Will Scudder ✓	
DDC	Q44 Scudder	
EXAMINER		
NOTATION		
BY		
DISTRIBUTION AVAILABILITY		
Dist.	AVAIL	Scudder
A		

UNCLASSIFIED

SECURITY CLASSIFICATION OF THIS PAGE (When Data Entered)

TABLE OF CONTENTS

	<u>PAGE</u>
Figure Captions (Page No.)	4
I Introduction	5
II Instrument Design	6
III Techniques Used in Calibration	8
IV Results	10
Table 1	14
Table 2	15
Acknowledgements	16
Figures 1-11	17 - 27
Appendix A	28
Appendix B	30
Appendix C	31
Computer Program Used for Monte Carlo Computations	
References	42

FIGURE CAPTIONS

- Figure 1. The SSJ/3 instrument and associated electronic
(17) boards. The rectangular slits are entrance apertures for electrons. Behind the small circular hole is a UV detector that causes the channeltron acceleration voltage to be turned off when viewing the sun.
- Figure 2. Detailed phtotgraph of the SSJ/3 head assembly board.
(18) a $\frac{1}{2}$ " block is also shown for comparison. The narrowly separated plates select the high-energy electrons. The widely separated plates select the lower energy electrons.
- Figure 3. Detailed schematic sketch of a detector assembly.
(19) Also given are the relevant dimensions for each set of plates.
- Figure 4. Schematic of the electronic logic used in SSJ/3.
(20)
- Figure 5. Comparison between measured and Monte-Carlo results
(21) for a normally incident beam. Energies are off-set for ease of display.
- Figure 6. Angular response of the high-energy plates in the
(22) R-plane (α).
- Figure 7. Angular response of the low energy plates in the
(23) R-plane (α).
- Figure 8. Angular response of the high-energy plates in the
(24) plane parallel to the plates (β).
- Figure 9. Angular response of the low energy plates in the
(25) plane parallel to the plates (β).
- Figure 10. Theoretical response of the high-energy plates to
(26) an isotropic incident flux. Use Table 2 for channel 8 mid-point energy. Final normalization is also shown.
- Figure 11. Theoretical response of the low energy plates to
(27) an isotropic incident flux. Use Table 2 for channel 9 mid-point energy. Final normalization is also shown.

I. INTRODUCTION

The calibration of the SSJ/3 sensor was carried out using both experimental and theoretical techniques. Experimental measurements were compared with predictions from a Monte Carlo particle tracing code and from analytic approximations.

In Section II instrument design is discussed. Section III described techniques used in calibration while Section IV describes the logic used to obtain the final normalization values.

II. INSTRUMENT DESIGN

Introduction. The SSJ/3 instrument package is shown in Figures 1 and 2. Figure 1 shows the instrument case and the associated electronic boards. The apertures on the case are directly in front of the particle collimators that are shown in the bottom of Figure 2. Behind the collimators are curved cylindrical plates. The plate separation and the applied voltage determine the energy band of the transmitted electrons. The electrons, after passing through the exit collimator, are detected by the C-shaped Channeltron Electron Multiplier detectors that are also shown in Figure 2.

Head Assembly. Electrostatic analyzers (ESA's) select charged particles by applying a voltage between two concentric plates. The SSJ/3 instrument uses two sets of cylindrical concentric plates as shown in Figure 2. Charged particles of the proper sign and energy have trajectories that are almost parallel to the plate surfaces. Particles of greater or lesser energy impinge on the plate surfaces. The mean energy E can be easily derived by requiring a balance between electrostatic and centrifugal accelerations. For plates of radii r_1 and r_2 ($r_2 > r_1$) and an applied voltage difference of V , E is given by

$$E = \frac{eV}{2 \ln(r_2/r_1)} \quad (1)$$

If V is fixed then the detected energy is determined by the ratio of r_2 to r_1 . This explains the larger plate separation, ΔR , for the lower energy detector assembly as tabulated in Figure 3. The sector angle of the plates and their separations, together with aperture and exit slits, determine the

transmission efficiency. Additional baffles are placed in the aperture assembly to eliminate sunlight (UV) scatter into the detectors.

Behind the exit aperture, the two channeltrons are mounted as shown in the lower righthand corner of Figure 2. Electrons impinging on the cone-shaped area produce secondaries which cascade through the channeltron producing a detectable pulse at the end. This pulse is then processed by the instrument's internal electronics. Channeltron operating lifetime is extended by shutting off the accelerating potential whenever the instrument is looking at the sun. This is done by a small phototransistor mounted adjacent to the instrument apertures. See Figure 1. In Figure 3 is a schematic representation of the SSJ/3 head assemblies and gives the relevant dimensional values.

Electronic Logic. Figure 4 shows the electronic logic. The channeltron outputs (DET L and DET H) are amplified and then counted in nine-bit logarithmic counters. A complete 16-channel energy spectrum is read out every second. Appendix A describes in detail the conversion of the logarithmic counter to decimal form. The same programmable power supply is used for biasing both sets of plates. The voltage difference for each set of plates is obtained by applying $\pm V/2$ to each plate.

III. TECHNIQUES USED IN CALIBRATION

Experimental. Experimental calibrations were made using accelerated electrons from a Tritium source. After acceleration by an applied voltage, the beam was collimated so that a mono-energetic, unidirectional source was incident on the instrument apertures. A turntable enclosed in a vacuum system provided mobility for angular response measurements. The beam was found to have an energy dispersion which was negligible in comparison with the instrument's response. By changing the applied voltage various energies could be selected.

Theoretical Approximations. Geometric considerations lead to the following results: 1) If a and b are the heights of the entrance and exit apertures of the collimator and ℓ is the separation then between them such that $\ell \gg a + b$, then the angular resolution, $\Delta\beta$, is to a good approximation given by $\Delta\beta \approx (a + b)/\ell$. This approximation works well for the direction parallel to the plates, but not for the orthogonal component. 2) The geometric factor ($\text{cm}^2\text{-sec}$) for a long rectangular collimator is approximated by

$$G = \frac{A_1 \times A_2}{\ell^2}$$

A_1 = area of collimator entrance aperture

A_2 = area of collimator exit aperture

ℓ = distance between apertures

This formula provides a rapid means of obtaining a "ballpark" estimate for the geometric factor of a rectangular collimator. We used, however, the exact expression given in Appendix B in deriving our final results.

Monte Carlo Program. In Appendix C is a listing of the Monte Carlo computer code used to analyze instrument response. The basic idea is to trace electrons through the instrument to determine if they hit the channeltron. In this manner the

effect of design can immediately be recognized.

Input data includes aperture geometry, plate radii, arc length of plates, plate voltage, channeltron size, and the position of the aperture and channeltrons relative to the plates. A retarding potential can also be inputed which impedes secondary electrons produced in the plates from hitting the channeltrons. Provision has also been made to examine elastic scattering off the plate surfaces. This feature will not be used.

Let us now consider an isotropic flux, J , incident on the outside aperture. The number of incident particles per unit area is given by

$$dN = J \sin\theta \cos\theta d\theta \quad (1)$$

or if R is a random number over the interval 0-1 then the relation

$$\theta = \frac{1}{2}\cos^{-1}(1-2R) \quad (2)$$

generates the appropriate angular distribution of incident particles.

As a test we generated 6×10^5 particles through the high-energy collimator using equation (2). The theoretically calculated geometric factor for this collimator (1.8 cm high \times 0.2 cm wide \times 1.15 cm long) is $0.0622 \text{ cm}^2/\text{sr}$ (Appendix B). The "measured" geometrical factor using particle tracing was found to be $0.0624 \text{ cm}^2/\text{sr}$ which agrees with the theoretical value to within 0.32%. This result confirms that the computer code was properly simulating an incident isotropic flux through the collimator.

IV. RESULTS

The Method. Instrument calibration is determined by comparing the predicted (Monte Carlo) response curves with the measured ones. First, we look at the energy resolution for a normally incident beam. Then angular response is examined in directions parallel and perpendicular to the plates. After showing substantial agreement with experimental data, the Monte Carlo code is used to calculate the final normalizations for an incident, isotropic flux. Comparisons are made with results from approximate analytic techniques. Channeltron detection efficiency as a function of incident electron energy is also discussed and included.

Throughout this section we use energy channels 8 and 9 to determine the response properties of the two head assemblies.

Energy Resolution. In Figure 5 the Monte-Carlo and experimental results are shown for a normally incident electron beam. The beam energy was systematically scanned across the channel to obtain the energy response curve. It is seen from Figure 5 that the Monte Carlo and experimental results are in excellent agreement.

Angular Response. Figure 6 shows the angular response (α) of the high energy plates in the plane perpendicular to the plates (R-plane). In this case the measured resolution is somewhat wider than that predicted by Monte Carlo. This effect is probably due to scattering off the plate surface. Figure 7 shows a similar response curve for the low-energy plates. Observe that there are fewer measured particles than predicted at large positive angles. This effect is probably from fringe electric field resulting from larger plate separation. See Figure 2. The triangular shape of the theoretical response curve indicates that the front collimator

is the dominant determinant of the angular response.

Now we look at the angular response (β) in the plane parallel to the plate surfaces. All angular response curves are determined at the central (peak) channel energy. Figure 8 shows the appropriate curves for the high energy (narrowly separated) plates. Note that while the resolution is in excellent agreement, there is a systematic shift of about 2.5° . Because the resolution is about 8.0° , we do not consider this error as being serious. Figure 9 shows similar curves for the low energy (widely separated) plates. Here there is also a systematic shift of about 1.25° . Note that for both angular scans the measured resolutions for the low energy plates are less than the predicted ones. This is opposite to what one would normally expect and indicates a slight systematic error.

Final Normalizations. The final normalizations were determined using the Monte Carlo program. As described previously, an isotropic flux is taken incident on the front aperture. One thousand electrons are traced through the plates at each energy. Figure 10 and 11 show the results for channels 8 and 9 respectively. The ordinate represents the percentage of electrons that are detected after leaving the collimator (i.e. the transmission efficiency through the plates). The integral of this curve times the aperture G-factor gives the final normalizations.

For an incident flux J the count rate (CR) is given by

$$JG = CR$$

where G is the normalization factor in $\text{cm}^2/\text{sr}/\text{ev}$. The G-factor can be approximated by

$$G \approx A\Omega \Delta E$$

A = area of entrance aperture

Ω = acceptance solid-angle

E = energy bandwidth

Dividing by the center energy E we have

$$H = G/E \approx A\Omega \frac{\Delta E}{E} .$$

Now since A, Ω and $\Delta E/E$ are constant for each set of plates, then this one number H characterizes the normalization for all channels. For the high-energy (narrowly separated plates) channels $H = 1.30 \times 10^{-4} \text{ cm}^2/\text{sr}$. For the low-energy (widely-separated plates) $H = 4.3 \times 10^{-5} \text{ cm}^2/\text{sr}$.

We now compare this result with an approximate analytic approach. In this approach it is assumed that the energy and angular response curves are independent gaussian distributions. The final normalization is the integral product of these distributions. The result is

$$H = 1.20 A\varepsilon R_0 \Delta\alpha\Delta\beta$$

where A is the aperture area, R_0 is the channeltron detection efficiency (at $E \sim 1 \text{ keV}$, $\varepsilon = 1$), R_0 is $\Delta E/E$, $\Delta\alpha$ and $\Delta\beta$ are the FWHM (full-width half maximum) of the angular response curves.

Using the measured results tabulated in Table 1, this approximation gives us $H = 6.8 \times 10^{-5} \text{ cm}^2/\text{sr}$ for the high energy plates and $H = 5.55 \times 10^{-5} \text{ cm}^2/\text{sr}$ for the low energy plates. Note, however, that energy and angular resolutions are not independent for this particular electrostatic analyzer, contrary to the assumptions in the approximate approach.

A wide collimator allows more electrons at various energies to reach the channeltrons. A narrow collimator allows fewer electrons to reach the detectors over a narrower energy bandwidth. This effect is seen by comparing Figure 5 with Figures 10 and 11. The energy resolution of the high-energy plates is 2.3 times greater for an isotropic flux than for a normally incident flux. For the low energy plates it is 1.5 times greater. We interpret this difference to be due to the collimator in front of the high energy plates having a G-factor 16 times that of the one in front of the low-energy plates. It is for this reason we consider the Monte Carlo normalization as more closely reflecting realistic fluxes.

The final normalizatin values for each energy channel as given in Table 2. Dividing the count rate by the approximate normalization gives the equivalent flux in electrons per $\text{cm}^2/\text{sr}/\text{ev/sec}$. The channeltron efficiencies were obtained from Archuleter and DeForest (1971). For $1 \text{ keV} \leq E \leq 50 \text{ MeV}$, $\epsilon = 1.0 - 2.0/(3.0 + 6.5/(E - 0.5) + 30.0/(E - 0.5)^3)$ where E is expressed in keV. For $10 \text{ ev} \leq E \leq 70 \text{ eV}$ ϵ was taken to be

$$\epsilon = 0.10 E^{0.515} \quad (\text{E in ev})$$

Note that the midpoint energies in Figures 10 and 11 ar not the same as in Table 2, which are the final calibrated values. This does not affect H , however, which is energy-independent. The stated errors in Table 2 for the various energy channels are a best estimate from electronic and experimental uncertainties.

TABLE 1

Measured Energy and Angular Resolutions With a
Monoenergetic and Unidirectional Electron Beam

	<u>Channels 1-8</u>	<u>Channels 9-16</u>
$\Delta\alpha$	$1.6 \pm 0.2^\circ$	$3.7 \pm 0.7^\circ$
$\Delta\beta$	$8.0 \pm 0.8^\circ$	$4.75 \pm 0.08^\circ$
$\Delta E/E(R_0)$	$4.0 \pm 0.4\%$	$7.2 \pm 0.4\%$
G (Aperture)	$6.22 \times 10^{-2} \text{ cm}^2 \cdot \text{sr}$	$3.929 \times 10^{-3} \text{ cm}^2 \cdot \text{sr}$

TABLE 2
SSJ/3 Normalizations

$$H = 1.30 \times 10^{-4} \text{ cm}^2 \cdot \text{sr}$$

<u>Channel Number</u>	<u>Center Energy (eV)</u>	<u>Channeltron Efficiency ϵ</u>	$G = HE\epsilon$ <u>Normalization (G)</u> $HE\epsilon (\text{cm}^2 \cdot \text{sr} \cdot \text{eV})$
1	$20,000 \pm 3\%$	0.405	1.05×10^0
2	$13,700 \pm 3\%$	0.43	7.66×10^{-1}
3	$8,990 \pm 3\%$	0.48	5.59×10^{-1}
4	$5.500 \pm 3\%$	0.56	4.00×10^{-1}
5	$3.790 \pm 3\%$	0.66	3.25×10^{-1}
6	$2,290 \pm 3\%$	0.83	2.47×10^{-1}
7	$1,590 \pm 5\%$	0.94	1.94×10^{-1}
8	$1,060 \pm 6\%$	0.99	1.36×10^{-1}

$$H = 4.3 \times 10^{-5} \text{ cm}^2 \cdot \text{sr}$$

9	$1,045 \pm 3\%$	1.00	4.49×10^{-2}
10	$661 \pm 3\%$	1.00	2.84×10^{-2}
11	$434 \pm 3\%$	1.00	1.86×10^{-2}
12	$264 \pm 3\%$	1.00	1.13×10^{-2}
13	$183 \pm 3\%$	1.00	7.86×10^{-3}
14	$110 \pm 3\%$	1.00	4.73×10^{-3}
15	$77 \pm 5\%$	1.00	3.31×10^{-3}
16	$51 \pm 6\%$.76	1.67×10^{-3}

ACKNOWLEDGEMENTS

We would like to express our appreciation to Dr. Davis Nelson of Aerospace Corporation who substantially contributed to many of the design features. In addition we would like to express our gratitude to the Space Physics Laboratory at Aerospace Corporation for the use of their calibration facilities.

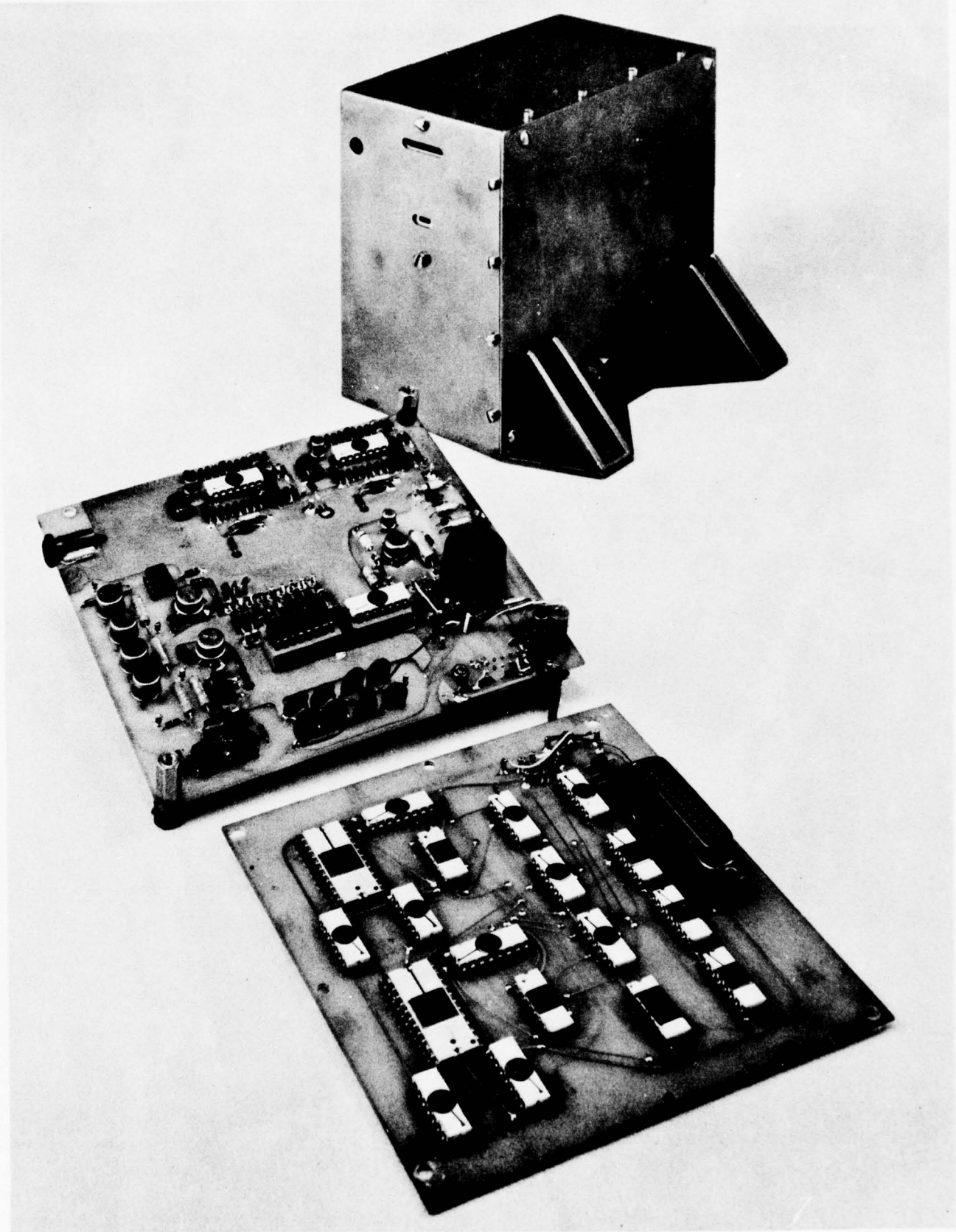


Fig. 1

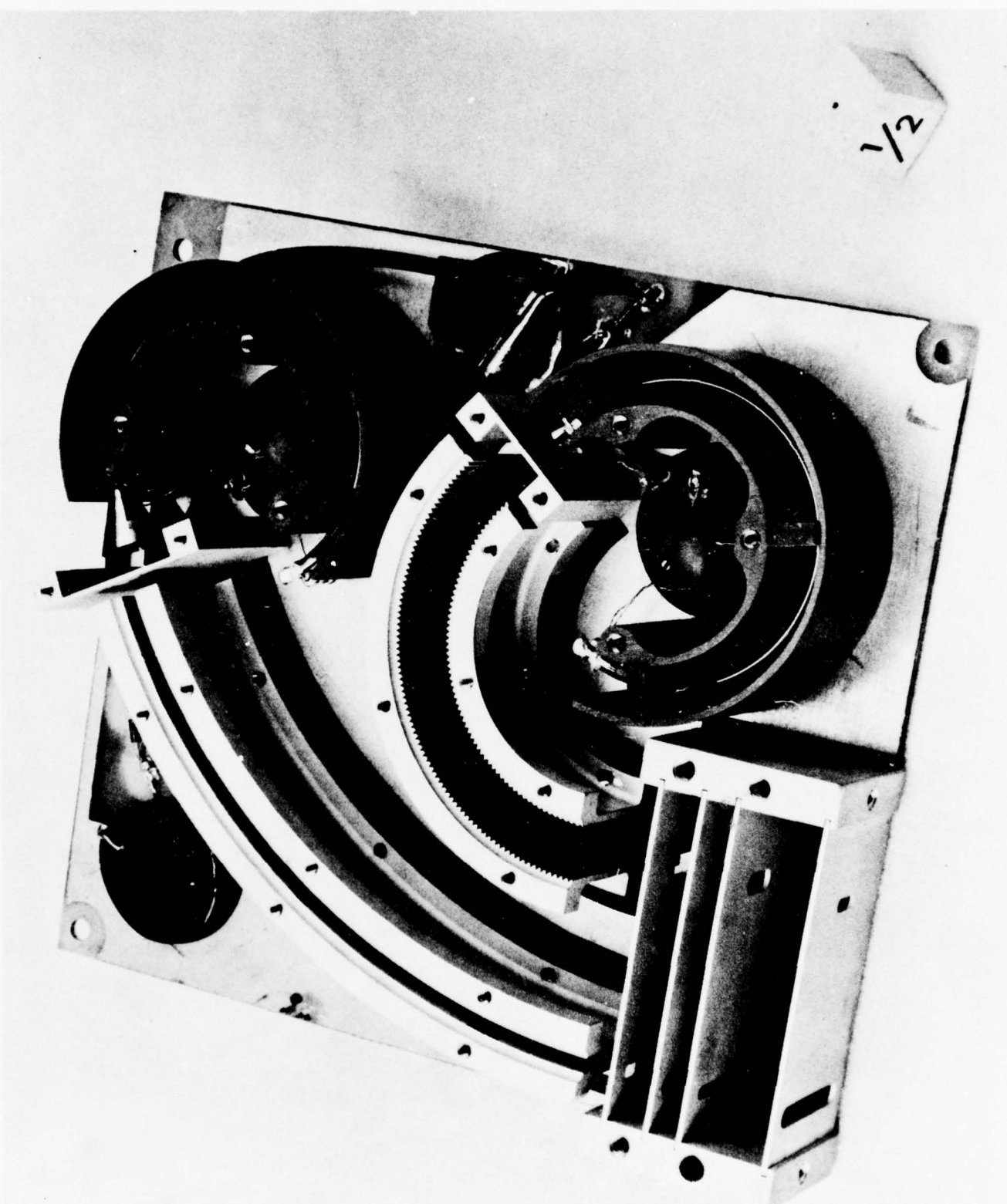


Fig. 2

SSJ / 3 ESA ASSEMBLY

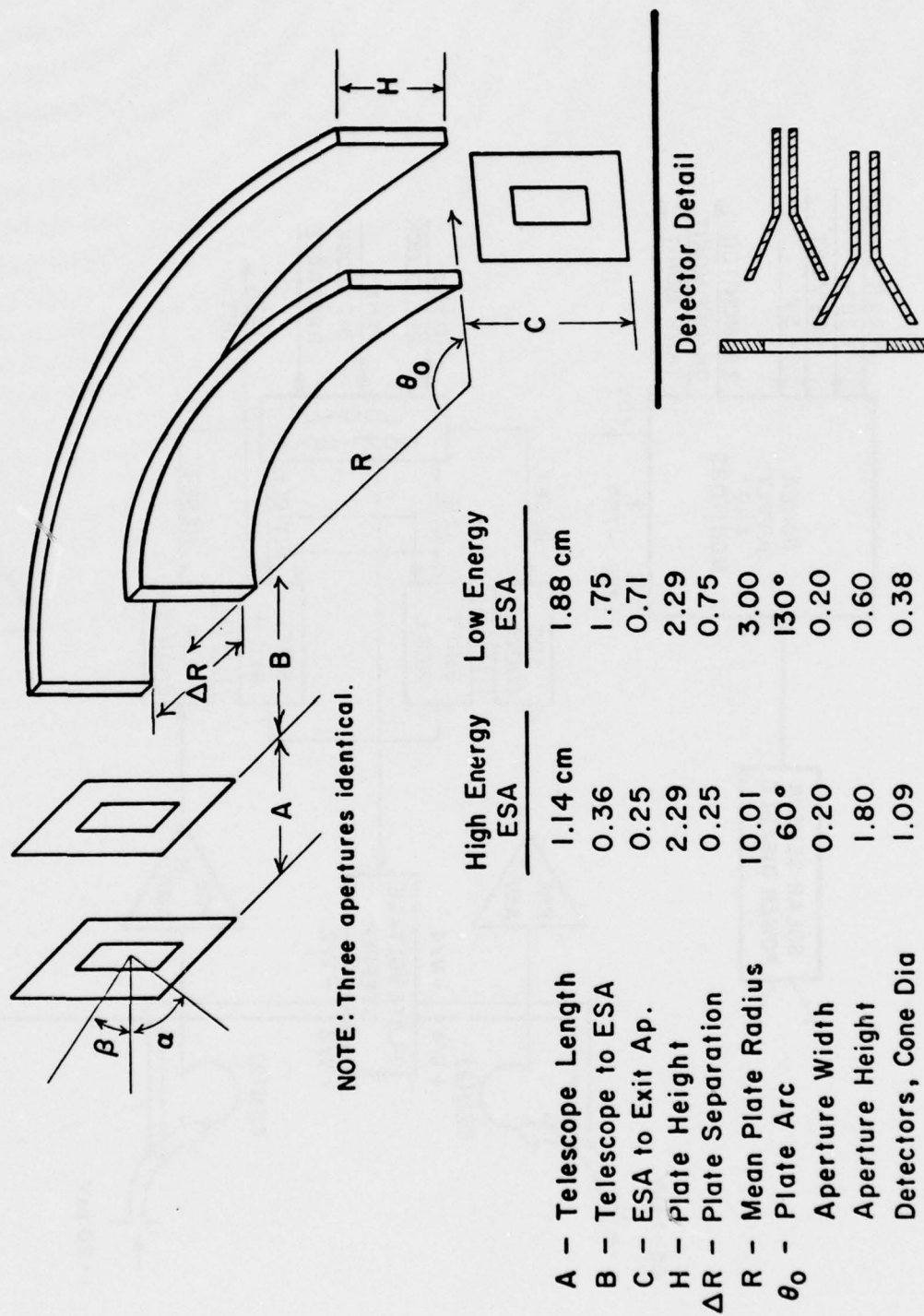


Fig. 3

SSJ / 3 BLOCK DIAGRAM

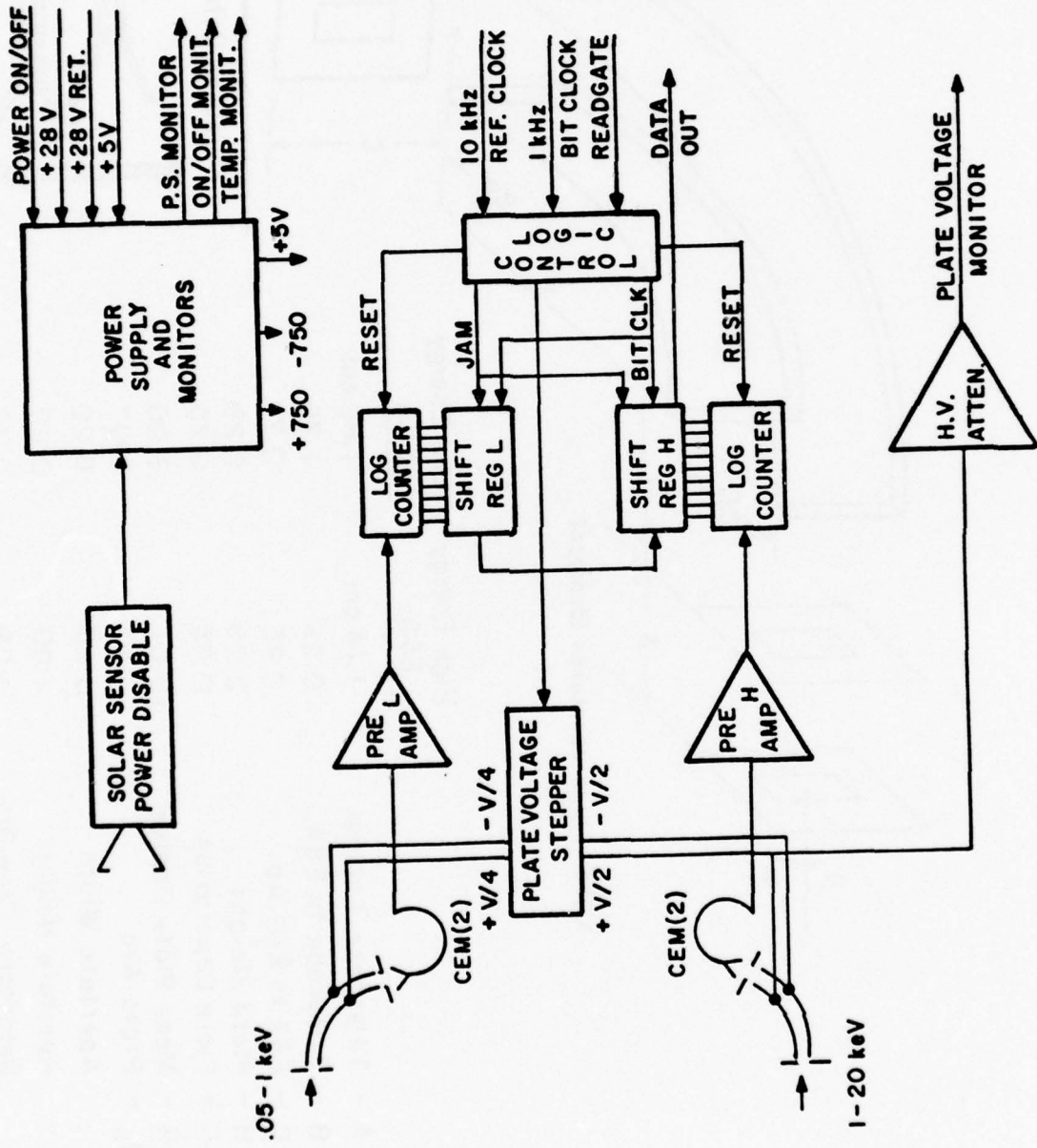


Fig. 4

ENERGY RESPONSE
NORMALLY INCIDENT AND MONOENERGETIC BEAM

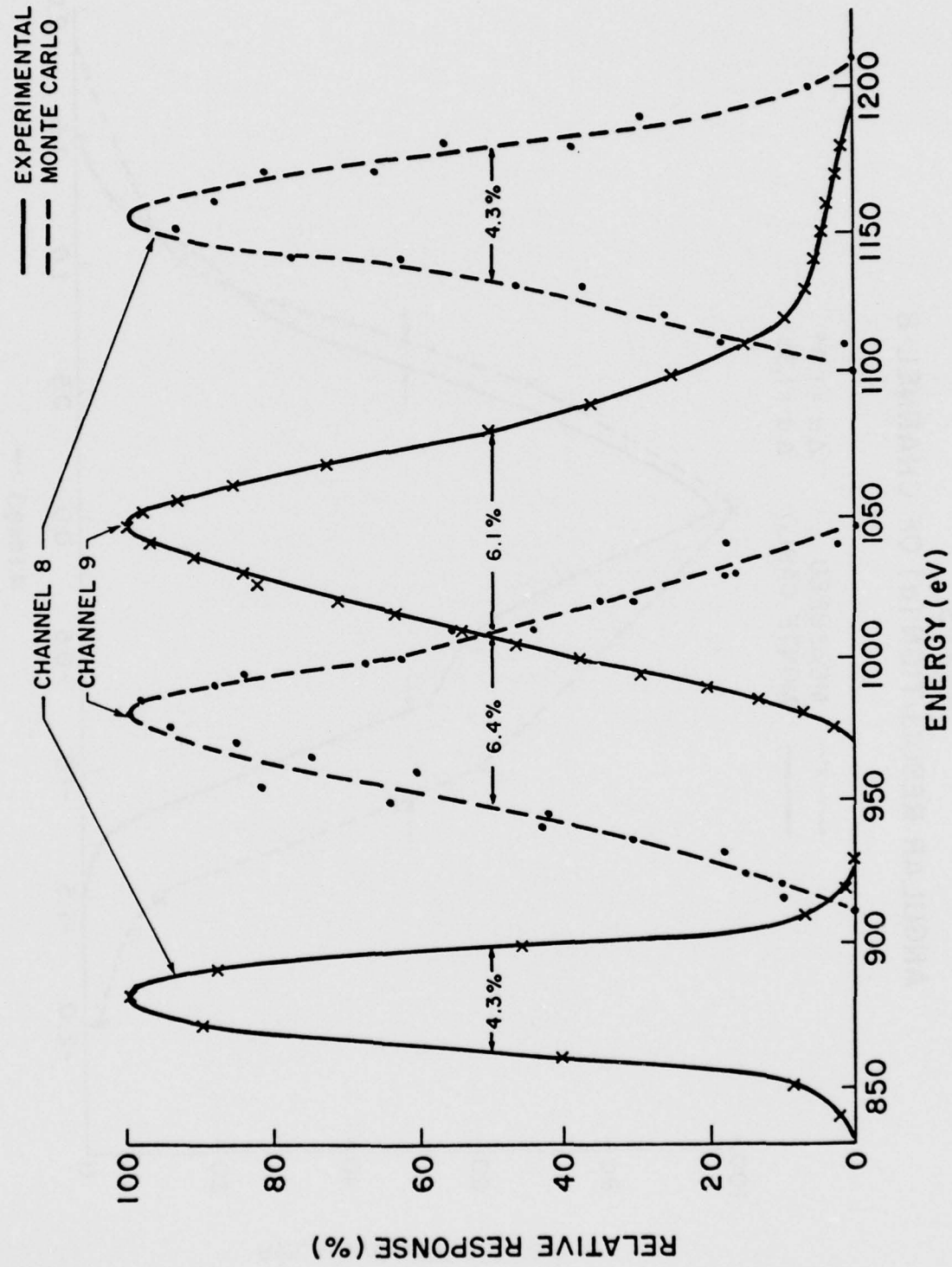


Fig. 5

SSJ/3
ANGULAR RESOLUTION (α) OF CHANNEL 8

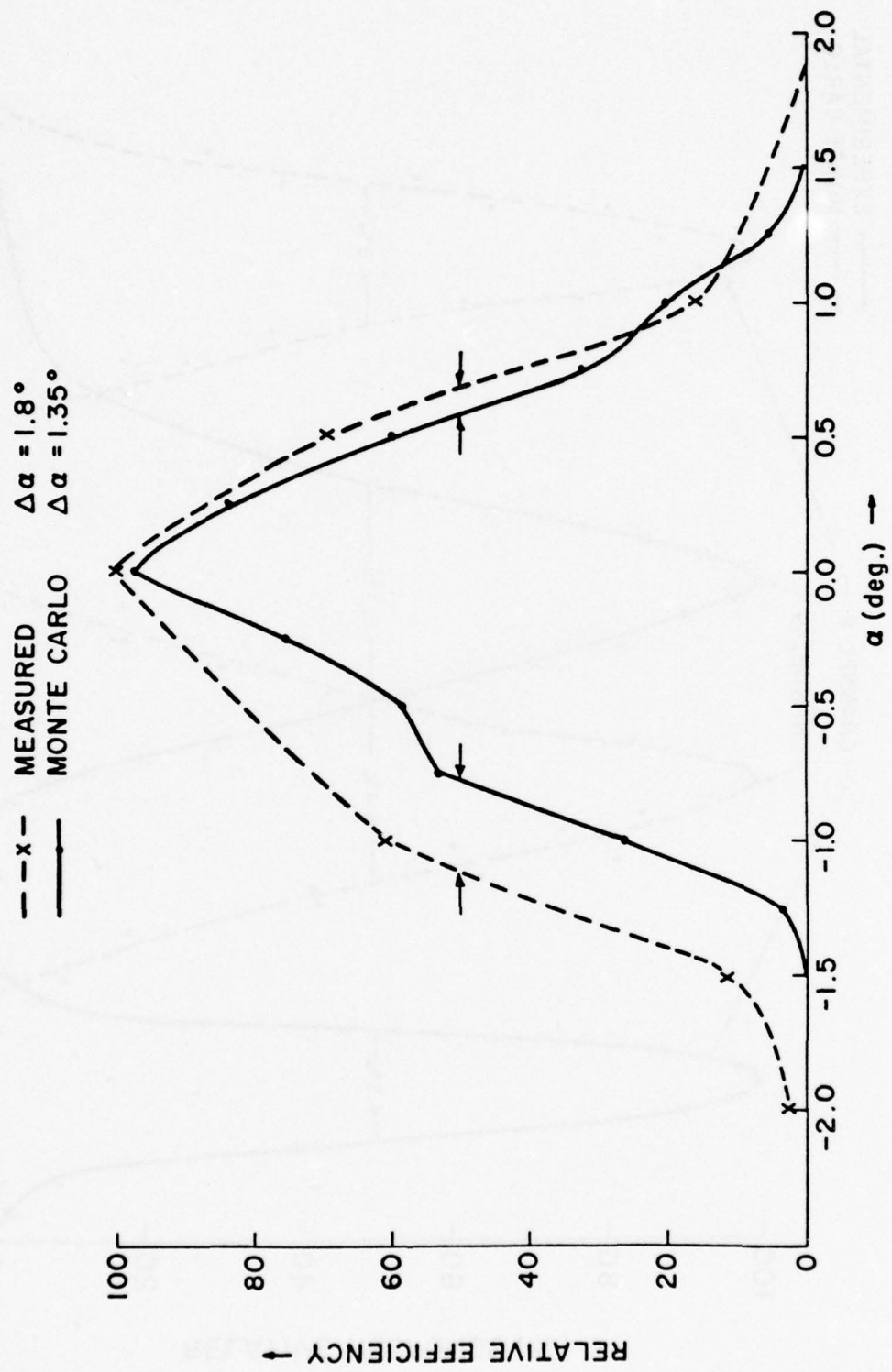


Fig. 6

ANGULAR RESOLUTION (α) OF SSJ/3
ENERGY CHANNEL 9

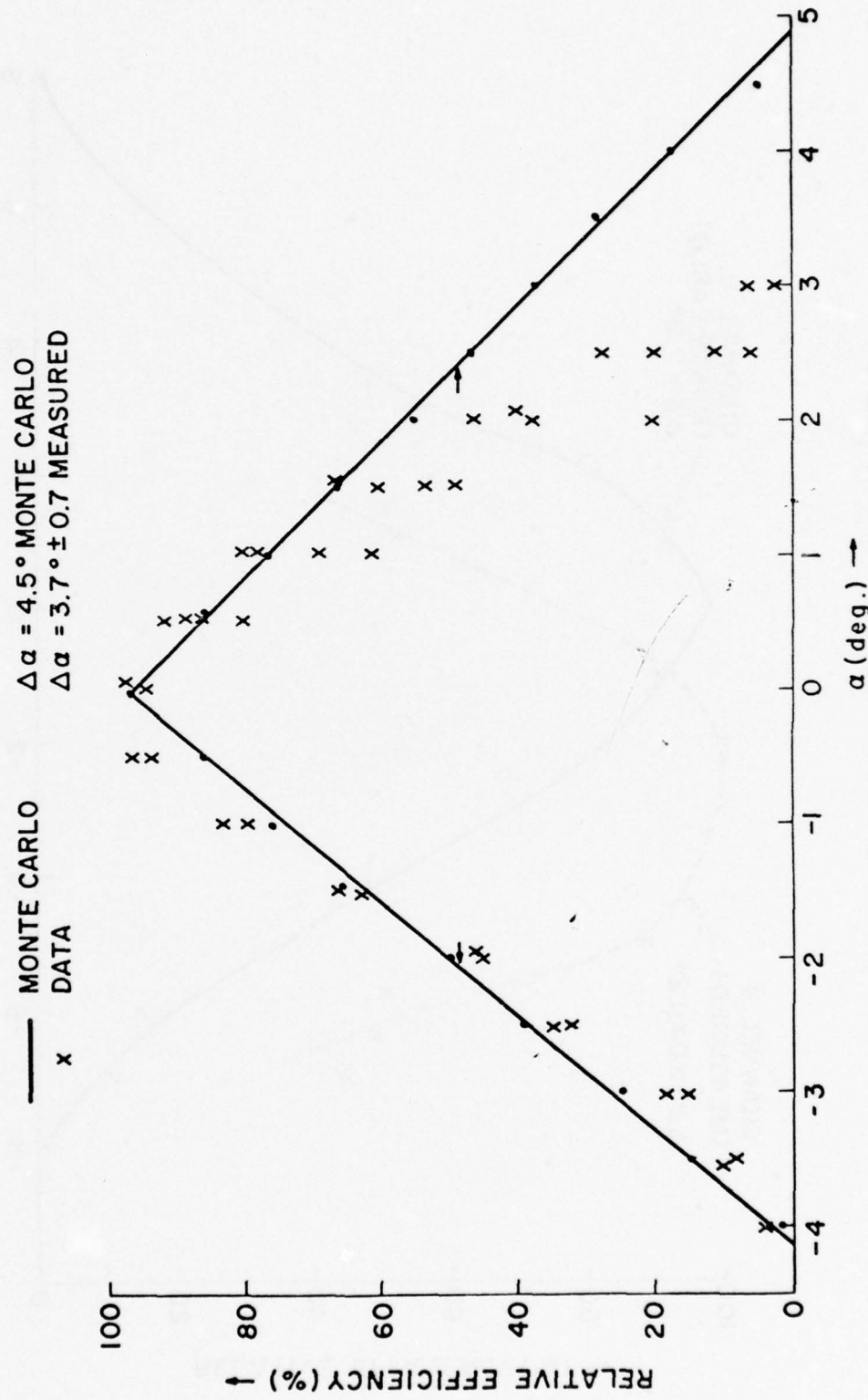


Fig. 7

SSJ / 3
ANGULAR RESOLUTION (β) OF CHANNEL 8

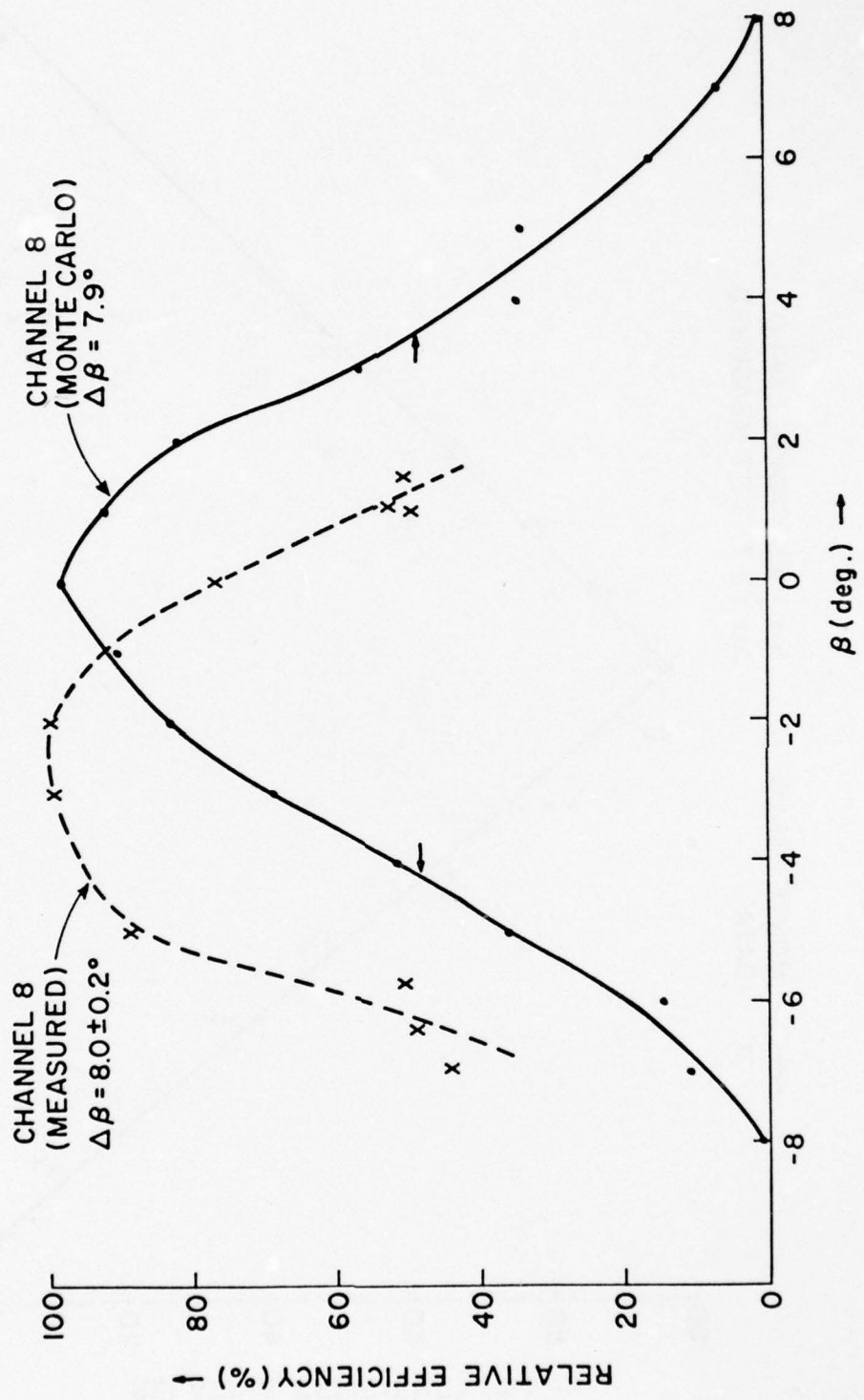


Fig. 8

ANGULAR RESOLUTION (β) OF SSJ/3
ENERGY CHANNEL 9

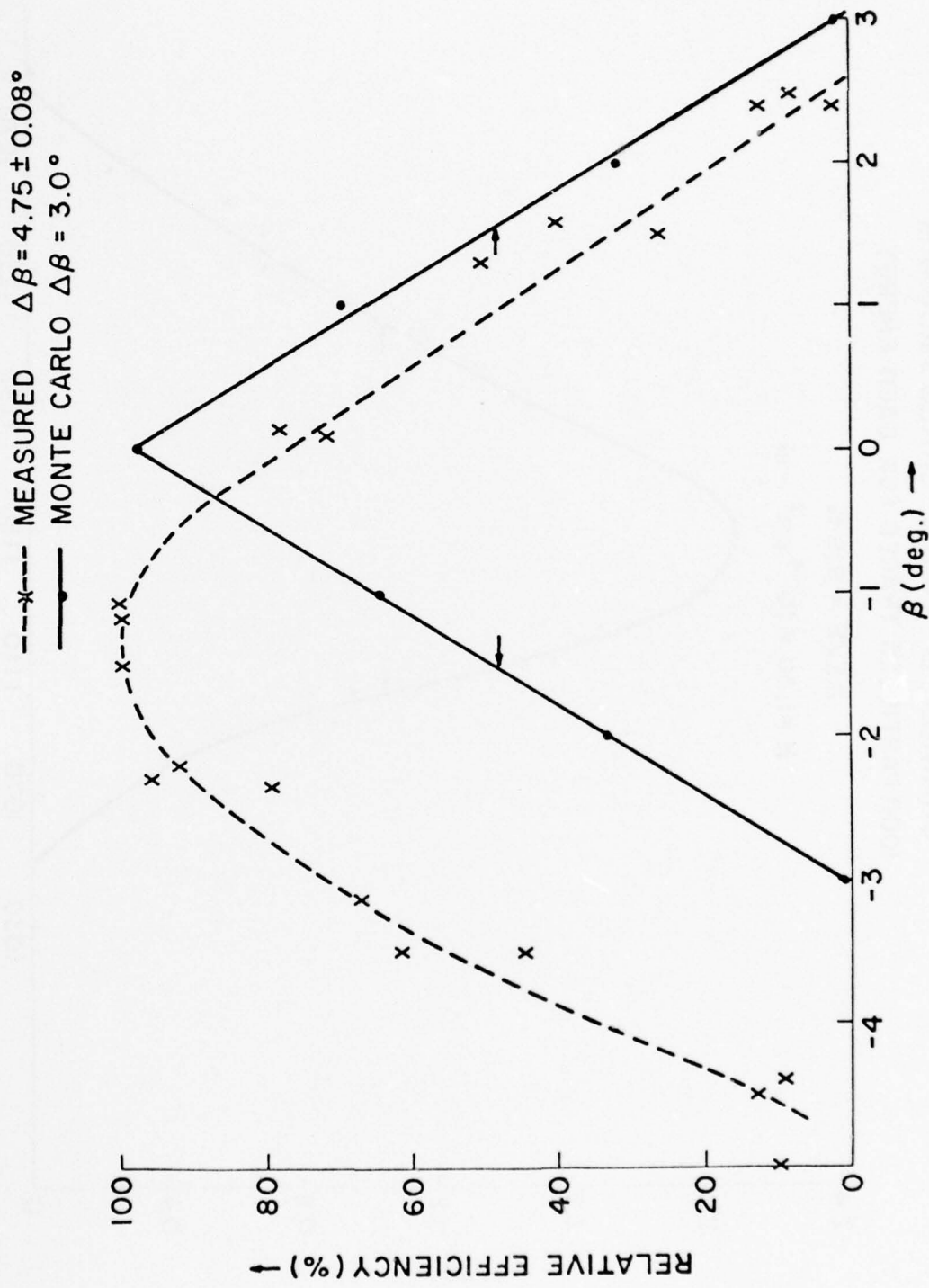


Fig. 9

ENERGY RESPONSE - ISOTROPIC INCIDENT FLUX
 CHANNEL 8 - MONTE CARLO PROGRAM
 1000 PARTICLES TRACED FOR EACH ENERGY

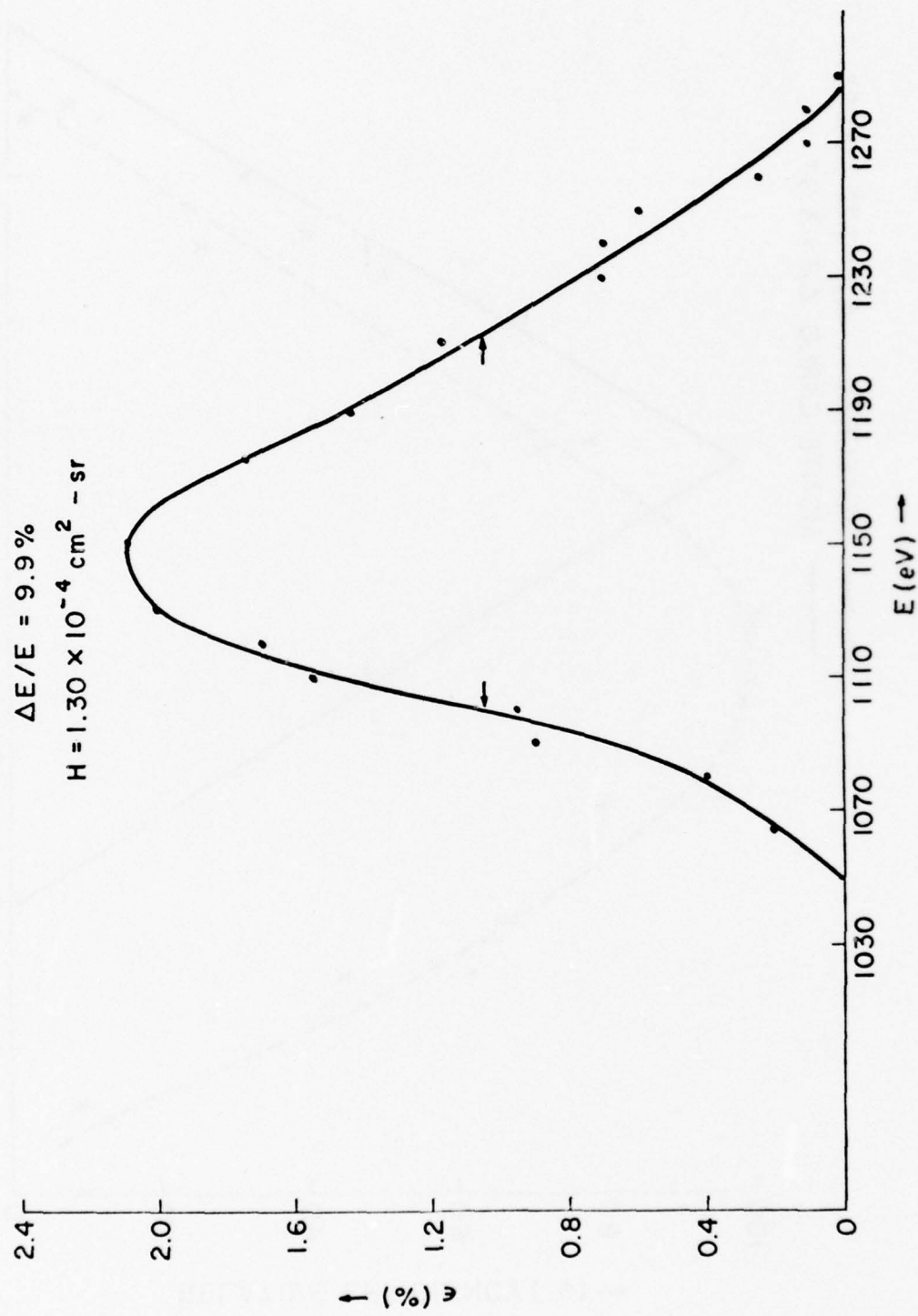


Fig. 10

ENERGY RESPONSE - ISOTROPIC INCIDENT FLUX
CHANNEL 9 - MONTE CARLO PROGRAM
1000 PARTICLES TRACED FOR EACH ENERGY

$$\Delta E/E = 9.2\%$$

$$H = 4.3 \times 10^{-5} \text{ cm}^2 \cdot \text{sr}$$

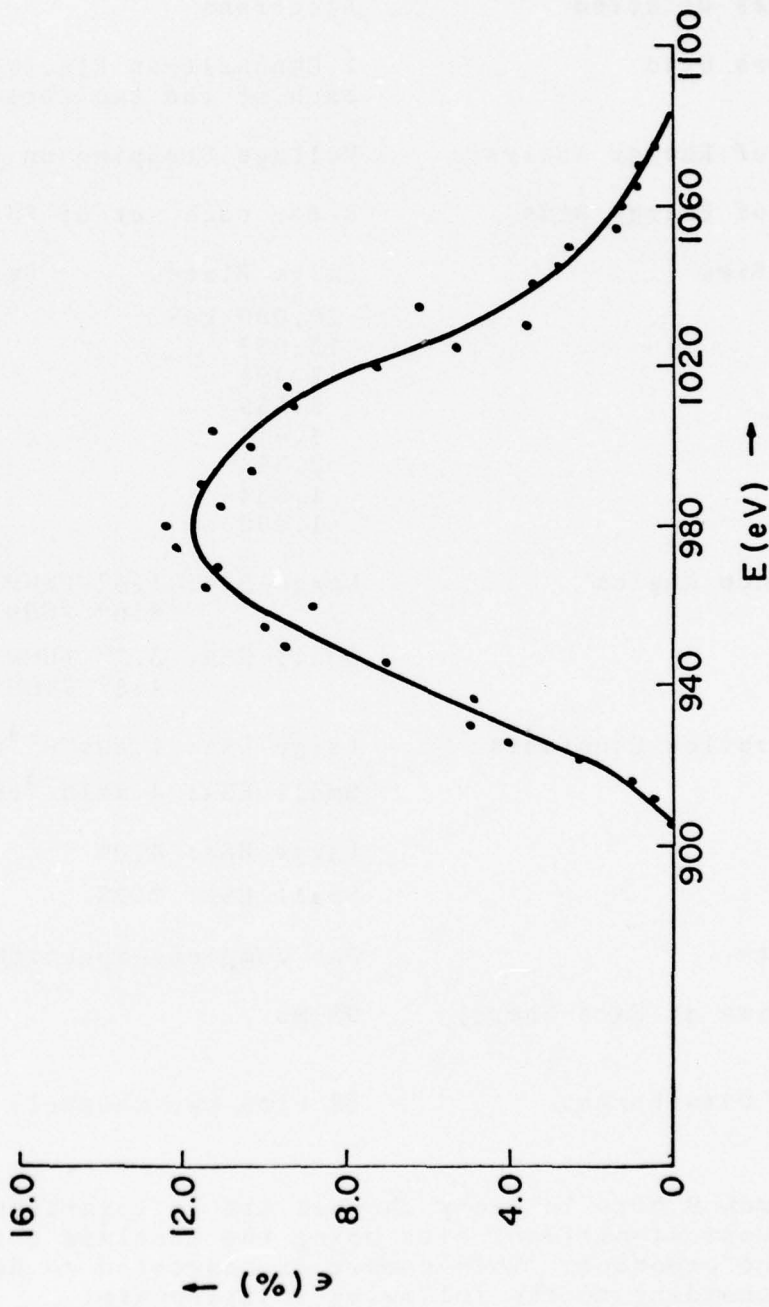


Fig. 11

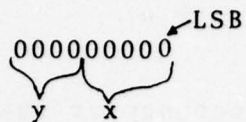
APPENDIX A
ELECTROSTATIC ANALYZER (ESA)
SSJ/3 OR GFE3

Summary of Characteristics

Particles Detected	Electrons	
Detectors Used	2 Channeltron Electron Multipliers for each of the two sets of ESA plates	
Method of Energy Analysis	Voltage Stepping on ESA plates	
Number of Energy Bins	8 for each set of ESA plates; total of 16	
Energy Bins	Large Plates	Small Plates
	20.000 keV	1.000 keV
	13.037	.652
	8.498	.425
	5.539	.277
	3.611	.181
	2.354	.118
	1.534	.077
	1.000	.050
Acceptance Angles	Large ESA: 1.6° FWHM across the apertures 8.0° FWHM along the apertures	
	Small ESA: 3.7° FWHM across the apertures 4.8° FWHM along the apertures	
Normalization Constants	Large ESA: $1.30 \times 10^{-4} \text{ cm}^2\text{-ster.}$ Small ESA: $4.3 \times 10^{-3} \text{ cm}^2\text{-ster.}$	
$\frac{\Delta E}{E}$	Large ESA: 4.0% Small ESA: 7.2%	
Data Rate	One complete Spectrum per second	
Dwell Time at Each Energy Level	98 ms.	
Digital Data Format	(9 bits per channel) x (16 channels) = 144 bits	

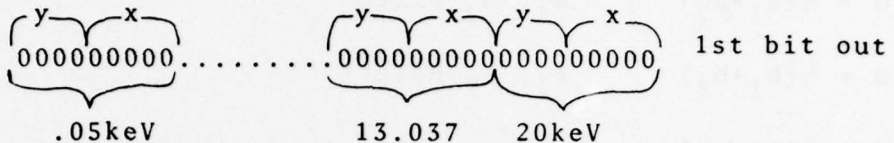
Note: Each 9 bits in every channel are in logarithmic form, the five least significant bits being the mantissa and the remaining four the exponent. This number is converted to decimal form according to the following relationship:

$$N = 2^y(x+32) - 33$$

where; 0000000000 

Data Readout

The first bit to be read out is the least significant bit (LSB) of the highest channel followed by the next to the highest one etc., i.e.:



[.....144 bits.....]

read out in one group
at the end of each second

Analog Monitors

Plate voltages: 5.0 volts to .25v

Power supply : 2.5v

Temperature : 2.5v at room temperature

Size

5.50in X 3.39in X 5.10in

Weight

3.046 lbs

Power Dissipation

.125 watts

APPENDIX B

The G-factor for a rectangular shaped collimator can be calculated exactly (Rothwell and Moomey, 1972).

With the front and rear apertures having the dimensions (a_1, b_1) and (a_2, b_2) respectively, one can define

$$\alpha = \frac{1}{2}(a_1 + a_2) \quad a_1, a_2 \text{ width}$$

$$\beta = \frac{1}{2}(b_1 + b_2) \quad b_1, b_2 \text{ height}$$

$$\gamma = \frac{1}{2}(a_1 - a_2)$$

$$\delta = \frac{1}{2}(b_1 - b_2)$$

If the collimator has a length L then

$$G = L^2 \ln \left[\frac{\frac{L^2 + \alpha^2 + \delta^2}{L^2 + \alpha^2 + \beta^2} \cdot \frac{L^2 + \gamma^2 + \beta^2}{L^2 + \gamma^2 + \delta^2}}{} \right] \\ + F(\alpha, \beta) + F(\gamma, \delta) - F(\alpha, \delta) - F(\gamma, \beta)$$

where $F(\alpha, \beta) = F(\alpha, \beta) + F(\beta, \alpha)$

$$F(\alpha, \beta) = 2\beta(L^2 + \alpha^2)^{\frac{1}{2}} \tan^{-1} \left[\frac{\beta}{(L^2 + \alpha^2)^{\frac{1}{2}}} \right]$$

This expression is consistent with that given by Willis and Thomas (1972) and by Sullivan (1971) (with a corrected typographical error).

APPENDIX C

Listing of computer code that was used for the Monte-Carlo computations.

```

PROGRAM ESAPLTS(INFUT,OUTPUT)          10
    DIMENSION DAT(24),EFF(200),EE(200),EG(200),AMAT(10,10),S   11
+UM1(10)                                11
    DIMENSION THH(100),AX(100),THM(100)      12
COMMON/F1/EFF,EG,DELE,N5,GINT           13
R2(X)=A*X+B                            14
F(X,Y,AL)=2.0*Y*SQRT(AL**2+X**2)*ATAN(Y/SQRT(AL**2+X**2))  15
N5=60                                    16
N7=N5/6                                  17
N9=5                                     18
N11=30                                    19
N12=N11/2                                20
AMP=1.66E-27                             21
Q0VMP=9.538E 07                         22
AME=9.1E-31                             23
QOME=1.7582E 11                         24
AA=180./3.141596                        25
CMTA=0.0                                 26
ELEC=8MELECTRON                         27
1  CONTINUE                               28
    CALL RANSET(TIME(DUM))                29
    CMTA=0.0                              30
C IF II=1 DC BACKGROUND CALCULATION BASE ON "LINE OF SIGHT" 31
C   IJ.NE. 0, AUTOMATICALLY ASSUMES PARAMETERS FOR L. FRANKS E 32
+SA                                       32
C IJ=2, SIMULATES ELECTRON GUN SCAN OF FRANKS ESA AS SHOWN IN F 33
+IG. 2 OF                                33
C HIS PAPER                               34
C II=1, DOES LINE OF SIGHT BACKGROUND CALCULATION 35
C K1=0, NO ELASTIC SCATTERING OFF OF ESA PLATES 36
C K1=1, MORE THAN 1 SCATTERING OFF OF ESA PLATES PER ELECTRON A 37
+S DEFINED                               37
C BY K2 (INNER PLATE)                  38
C K1=2, 1/K2X100 PER CENT SCATTERING OFF OF ESA PLATES (INNEF P 39
+LATES)                                   39
C K1=3, SCATTERING OFF OF OUTER ESA PLATE AS DEFINED BY K9 40
C K1=4, SCATTERING OFF OF OUTER ESA PLATE AS DEFINED BY 1/K9X100 41
C K1=5, SCATTERING OFF OF BOTH PLATES,K2 TIMES INNER PLATE,K9 T 42
+IMES CFF                                42
C ATE                                    43
C K1=6,CATTERING OFF OF BOTH PLATES1/K2 INNER,1/K9 TIMES OUTER 44
+PLATE                                   44
C IF IK=0 INCIDENT FLUX IS ISOTROPIC 45
C IK=1 INCIDENT FLUX AT INCIDENT ANGLE ANGE 46
C IF IK=2 SCAN IN R-PLANE IN STEPS OF ANGE DEGREES 47
C IF IK=3 SCAN IN Z-PLANE IN STEPS OF ANGE DEGREES 48
C NOTE-- IF IK GE 2 INPUT DATA PACK CHANGES 49
    READ 4,II,IJ,K1,K2,K9,ANGA,ANG2,ANGD,IK,ANGE 50
4  FORMAT(5I5,3F7.2,I5,F7.2)              51
    PFINT 1900,IK,ANGE                     52
1900 FORMAT(1X,I5,F7.2)                  53

```

IF(K1.EQ.0) K7=1	54
IF(K1.EQ.1) K7=1	55
IF(K1.EQ.2) K7=1	56
IF(K1.EQ.3) K7=2	57
IF(K1.EQ.4) K7=3	58
IF(K1.EQ.5) K7=2	59
IF(K1.EQ.6) K7=3	60
IF(K1.EQ.0) K8=1	61
IF(K1.EQ.1) K8=2	62
IF(K1.EQ.2) K8=3	63
IF(K1.EQ.3) K8=1	64
IF(K1.EQ.4) K8=1	65
IF(K1.EQ.5) K8=2	66
IF(K1.EQ.6) K8=3	67
IF(K1.EQ.7) K7=2	68
IF(K1.EQ.7) K8=3	69
IF(K1.EQ.8) K7=3	70
IF(K1.EQ.8) K8=2	71
READ 3,(DAT(I),I=1,24)	72
3 FORMAT((12A6))	73
READ2,PART,POST	74
2 FORMAT(A8,F8.0)	75
PRINT 5,(DAT(I),I=1,24)	76
5 FORMAT(1H1,12A6/12A6)	77
IF(IJ.EQ.1) PRINT 10	78
10 FORMAT(1X,*BACKGROUND CALCULATION*)	79
IF(IK.EQ.1) PRINT 12,ANGE	80
12 FORMAT(1X,* CONST. ANGLE SORT,ANGLE=*,F7.2,* DEG.*)	81
IF(PART.EQ.1 ELEC) AMP=AME	82
IF(PART.EQ.1 ELEC) QOVMF =-QOME	83
PRINT 6,PART	84
6 FORMAT(1X,*TRACING*,3X,A8/)	85
IF(PART.EQ.1 ELEC.AND.IJ.NE.0) POST=160.	86
IF(IJ.NE.0) PRINT 16	87
16 FORMAT(1X,* FRANKS ESA *)	88
IF(IJ.EQ.2) PRINT 18	89
18 FORMAT(1X,* ELECTRON GUN FLUX=2.0E 06 ELEC/CMSC/SEC*)	90
IF(K1.NE.0) PRINT 17,K1,K2,K9	91
17 FORMAT(1X,*ELASTIC SCATTERING OFF OF ESA PLATES ,*,	92
+*K1=*,IJ,	92
A * K2=*,IJ/1X,*IF K1=1 K2 SCATTERINGS PER PART., IFK1=2	93
+ EVERY OT	93
BHER K2 PART. MAY SCATTER*,*K5=*,IJ)	94
IF(K1.NE.0) PRINT 21,ANG2	95
IF(K1.NE.0) PRINT 19,ANGA	96
IF(K1.NE.0) PRINT 23,ANGD	97
19 FORMAT(1X,* MAX SCATTERING ANGLE OFF OF OUTER PLATE=*,F7.	98
+2,* DEG*)	98
21 FORMAT(1X,* MAX SCATTERING ANGLE OFF OF INNER PLATE=*,F7.	99
+2,* DEG*)	99
23 FORMAT(1X,*MAX. ANGLE FOR INELASTIC SCATTERING OFF OF OU	100
+TEF PLATE	100

```

A=*,F7.2) 101
C SET-UP APERTURE AND CALCULATE ITS G-FACTOR 101
    READ 8,A1,B1,A2,B2,AL1,AL2, AL3,VOLT1,R5 102
    8   FORMAT(7F7.3,2F7.3) 103
    PRINT 11,A1,B1,A2,B2,AL1,AL2,AL3,VOLT1,R5,POST 104
    11  FORMAT(1X,*APERTUREDIMENSIONS*/1X,*FRONT WIDTH=*,F7.3,* C 105
        +M*,3X,*FR 106
        10NHTH=*,F7.3,* CM*,3X, *BACK WIDTH=*,F7.3,* CM*,3X,*BACK 107
        +HT=*,F7.3 107
        2,*CM*/1X,*LENGTH OF APER.=*,F7.3,* CM*,3X, *DIST BTWN APE 108
        +R AND FLA 108
        3TES=*,F7.3,* CM*/1X,*DIST BTWN PLATES AND CHANN.=*,F7.3,* 109
        + CM*,3X,* 109
        4BIAS VOLTAGE IN FRONT OF DETECT.=*,F7.1,* VOLTS*/1X,*CHAN 110
        +NELTRON R 110
        1ADIUS=*,F7.2,* CM*,* POST ACCELERATION=*,F8.0,*VOLTS*/) 111
        ALPHA=(A1+A2)/2.0 112
        BETA=(B1+B2)/2.0 113
        GAM=(A1-A2)/2.0 114
        DELTA=(B1-B2)/2.0 115
        G1=AL1**2+ALOG((AL1**2+ALPHA**2+DELTA**2)*(AL1**2+GAM**2+ 116
        +BETA**2)) 116
        1(AL1**2+ALPHA**2+BETA**2)/(AL1**2+GAM**2+DELTA**2)) 117
        G2=F(ALPHA,BETA,AL1)+F(BETA,ALPHA,AL1)+F(GAM,DELTA,AL1)+F 118
        +(DELTA,GA 118
        1M,AL1)-F(ALPHA,DELTA,AL1)-F(DELTA,ALPHA,AL1)-F(GAM,BETA,A 119
        +L1)-F(PET 119
        2A,GAM,AL1) 120
        G=G1+G2 121
        PRINT 13,G 122
    13  FORMAT(1X,*G-FACTOR FOR APERTURE=*,E10.4,* CMSQ-SR*) 123
        PRINT 15 124
    15  FORMAT(1X,*ESA PLATE DIMENSIONS*) 125
C R2A=RADIUS AT APERTURE 126
C R2B=RADIUS AT EXIT 127
    READ 7,R1,R2A,R2B,THE,VOLT,H,TOT,R9 128
    7   FORMAT(4F7.3, E10.2, F7.3,E10.4,F7.2) 129
    PRINT 9,R1,R2A,R2B,THE,VOLT,H,TOT,R9 130
    9   FORMAT(1X,*ZERO POTENTIAL RADIUS=*,F7.3,*CM*,3X,*RADIUS A 131
        +T POTENTI 131
        1AL V AT APERTURE=*,F7.3,* CM*,3X,*RADIUS AT POTENTIAL V A 132
        +T EXIT=*, 132
        2F7.3,* CM*/3X,*MAX. ANGLE OF PLATES=*,F7.2,* DEGS*,3X,*VO 133
        +LTAGE ON 133
        3 PLATES=*,1PE10.2,* VOLTS* /3X,*PLATE HEIGHT=*,0PF7.2,* 134
        +CM*, * N 134
        4NUMBER OF PARTICLES TRACED FOR EACH ENERGY=*,1PE10.2/1X,*D 135
        +INSTANCE 0 135
        5F CHANNELTRON FROM CENTER OF ESA AXIS=*,1PE10.2,* CM*) 136
        IF(PART.EQ.EIEC) VOLT ==VOLT 137
        THE=THE/AA 138

```

BEST AVAILABLE COPY

H=H*1.0E-02	139
ANGR=ANGA/AA	140
ANGC=ANG2/AA	141
ANGD=ANG0/AA	142
ANGE=ANGE/AA	143
R1=P1*1.0E-02	144
R2A=R2A*1.0E-02	145
R2B=R2B*1.0E-02	146
P5=R5*1.0E-02	147
R9=R9*1.0E-02	148
R=R2A	149
A=(R2B-R2A)/THE	150
WIC1=AES(R2A-R1)	151
RR=(R1+R2B)/2.0	152
A1=A1*1.0E-02	153
B1=B1*1.0E-02	154
A2=A2*1.0E-02	155
B2=B2*1.0E-02	156
AL1=AL1*1.0E-02	157
AL2=AL2*1.0E-02	158
AL3=AL3*1.0E-02	159
R6=RR-A1/2.0	160
R7=RR-A2/2.0	161
R8=RR+A2/2.0	162
IF(IJ.NE.0) R6=1.24E-01	163
IF(IJ.NE.0) R7=R6	164
IF(IJ.NE.0) R8=R6+A2	165
IF(IJ.EQ.2) THY=-5.0/AA	166
DELY=1.0/AA	167
THW=THY-DELY	168
THX=THE/2.0	169
R3=P2(THX)	170
GO TO 14	171
24 IF(IK.GE.2) READ 26,VOLT	172
IF(IK.GE.2) PRINT 29,VOLT	173
26 FORMAT(1PE10.2)	174
29 FORMAT(1X,* VOLTAGE ON PLATES=*,1PE10.2,* VOLTS*)	175
IF(PART.EQ.ELEC) VCLT =-VOLT	176
14 CONTINUE	177
C USING MKS SYSTEM--ENERGY IN JOULES	178
EE(1)=VOLT/2.0 ALOG(R3/R1)*1.6E-19	179
EE(1)=ABS(EE(1))	180
CONST=Q0VMP*VOLT	181
EA=EE(1)/1.6E-19	182
PRINT 31,EA	183
31 FORMAT(1X,*MEAN ENERGY=*,1PE10.2,*EV*)	184
IF(IK.LT.2) GO TO 34	185
THH(1)=-ANGE*N12	186
DO 33 I=1,N11	187
THH(I+1)=THH(I)+ANGE	188
THM(I)=THH(I)*AA	189

BEST AVAILABLE COPY

AX(I)=0.0	190
33 CCNTINUE	191
THH(N11+1)=THH(N11+1)*AA	192
GO TO 36	193
34 CONTINUE	194
DELE=0.005*EE(1)	195
EE(1)=0.9*EE(1)	196
DO 35 K=1,N5	197
EE(K+1)=EE(K)+DELE	198
35 CONTINUE	199
36 CONTINUE	200
DO 22 J=1,10	201
DO 22 K=1,10	202
AMAT(K,J)=0.0	203
22 CONTINUE	204
25 CONTINUE	205
THW=THW+DELY	206
THW=-4.0/AA	207
DO 600 K=1,N5	208
K13=1	209
37 CONTINUE	210
K4=0	211
N4=0	212
N6=0	213
K5=0	214
CNT=0.0	215
COUNT=0.0	216
CNTA=0.0	217
C DELT=TIME INTERVAL FOR EACH STEP	218
GO TO 40	219
38 IF(IK.GE.2) GO TO 202	220
40 CONTINUE	221
K3=0	222
N3=0	223
K11=0	224
K12=0	225
EX=EE(K)	226
IF(IK.GE.2) EE(K)=EA*1.6E-19	227
V=SQRT(2.*EE(K)/AMF)	228
C PULL OUT DEFOREST CARDS	229
R=R6+A1*RANF(DUM)	230
Z1=91*RANF(DUM)	231
C CHOOSE T1 SUCH THAT FOR J(FLUX) = CONST. T1 IS PICKED SIN(T1* +COS(T1))	232
C TIMES,, SIN FOR SOLID ANGLE COS FOR PROJECTED AREA	233
T1=ACOS(1.0-2.0*RANF(DUM))/2.0	234
T2=6.2831*RANF(DUM)	235
IF(IK.EQ.1) T1=AANGE	236
IF(IK.EQ.1) T2=0.0	237
IF(IK.EQ.2) T1=THH(K13)	238
IF(IK.EQ.2) T2=0.0	239

IF(IK.EQ.3) T1=THH(K13)	240
IF(IK.EQ.3) T2=1.5707	241
IF(IJ.EQ.2) T1=ABS(THW)	242
IF(IJ.EQ.2.AND.THW.GE.0.0) T2=180./AA	243
IF(IJ.EQ.2.AND.THW.LT.0.0) T2=0.0	244
Y1=0	245
VR=V*SIN(T1)*COS(T2)	246
VTT=V*COS(T1)	247
VZ=V*SIN(T1)*SIN(T2)	248
DT=AL1/VTT	249
R=R+VR*DT	250
Z1=Z1+VZ*DT	251
IF(Z1.GT.B2.OR.Z1.LT.0.0) GO TO 38	252
IF(R.GT.R8.OR.R.LT.R7) GO TO 38	253
CNTA=CNTA+1.0	254
DT=AL2/VTT	255
R=R+VR*DT	256
Z1=Z1+VZ*DT	257
IF(R.GE.R2A.OR.R.LE.R1) GO TO 202	258
ANGM=VTT*R	259
TT1=0.0	260
R3=R2(TT1)	261
CONTT=CONST ALOG(R3/R1)	262
CONSS=CONST	263
IF(II.EQ.1) CONSS=0.0	264
DELT=CONTT/(R1+R3)*2	265
DELT=3.E-01*V/DELT	266
DELT=3.1416*THE*(R1+R3)/2./V/2.0E 02	267
IF(DELT.LE.DELT) DELT=DELT	268
GO TO 20	269
27 CONTINUE	270
IF(K12.GT.0.OR.K11.GT.0) R=R+VR*DELT	271
GOTO 28	272
28 CONTINUE	273
R3=P2(TT1)	274
CONS2=(VTT**2-CONSS/ALCG(R3/R1))/R	275
R=R+VR*DELT+CONS2*DELT**2/2.0	276
VR=VR+CONS2*DELT	277
28 CONTINUE	278
VTT=ANGM/R	279
TT1=TT1+VTT*DELT/R	280
Z1=Z1+DELT*VZ	281
IF(Z1.LE.0.0.OR.Z1.GE.H) GOTO 202	282
IF(TT1.GE.THE) GO TO 400	283
IF(R.GT.R1.AND.R.LT.R3) GO TO 1700	284
GO TO 1800	285
1700 CONTINUE	286
K11=0	287
K12=0	288
GO TO 20	289
1800 CONTINUE	290

BEST AVAILABLE COPY

C	K1=1,2-----SCATTER OFF OF INNER SURFACE ONLY	291
C	K1=3,4-----SCATTER OFF OF OUTER SURFACE ONLY	292
	IF(R.GE.R3) GO TO 1300	293
	IF(R.LE.R1) GO TO 1400	294
	GO TO 202	295
1300	CONTINUE	296
	IF(K11.GT.0) GO TO 27	297
	K11=K11+1	298
	GO TO (202,1100,1200),K7	299
1400	CONTINUE	300
	IF(K12.GT.0) GO TO 27	301
	K12=K12+1	302
	GO TO (202,900,1000),K8	303
9000	CONTINUE	304
	N3=N3+1	305
	IF(N3.GT.K9) GO TO 202	306
	VD=ABS(VR)	307
	THP=ATAN(VD/VTT)	308
	IF(ABS(THP).GT.ANGC) GO TO 1500	309
	VR=-VR	310
	GO TO 27	311
10000	CONTINUE	312
	VD=ABS(VR)	313
	THP=ATAN(VD/VTT)	314
	N6=N6+1	315
	IF(ABS(THP).GT.ANGC) GO TO 1500	316
	VR=-VR	317
	GO TO 201	318
11000	CONTINUE	319
	VD=ABS(VR)	320
	K3=K3+1	321
	IF(K3.GT.K2) GO TO 202	322
	THP= ATAN(VR/VTT)	323
	IF(ABS(THP).GT.ANGC) GO TO 202	324
	IF(ABS(THP).GT.ANGB) GO TO 1600	325
	VR=-VR	326
	GO TO 27	327
12000	CONTINUE	328
	VD=ABS(VR)	329
	K4=K4+1	330
	THP= ATAN(VR/VTT)	331
	IF(ABS(THP).GT.ANGC) GO TO 202	332
	IF(ABS(THP).GT.ANGB) GO TO 1600	333
	VR=-VR	334
	GO TO 200	335
15000	CONTINUE	336
	EX=EX *(1.0-RANF(BUM))**(1.0/1.35)	337
	VA=SQRT(2.0*EX/AMP)	338
	VR=VA*SIN(THP)	339
	VTT=VA*COS(THP)	340
	IF(K8.EQ.3) GO TO 201	341

GO TO 27	342
1600 CONTINUE	343
EX=EX *(1.0-RANF(DUM))** (1.0/1.35)	344
VA=SQRT(2.0*EX/AMP)	345
VR=-VA*SIN(THP)	346
VTT=VA*COS(THP)	347
IF(K7.EQ.3) GO TO 200	348
GO TO 27	349
200 CONTINUE	350
IAB=MDC(K4,K2)	351
IF(IAB.EQ.0) K4=0	352
K5=K4	353
IF(IAB.EQ.0) GO TO 27	354
GO TO 202	355
201 CONTINUE	356
IAC=MDC(N6,K9)	357
IF(IAC.EQ.0) N6=0	358
N4=N6	359
IF(IAC.EQ.0) GO TO 27	360
202 CONTINUE	361
CNT=CNT+1	362
IF(CNT.GE.TOT) GO TO 500	353
GO TO 40	364
400 CONTINUE	365
C SET UP MATRIX AT EXIT APERTURE OF FLATES	366
DO 420 N=1,N9	367
IF(Z1.GE.(N-1)*H/N9.AND.Z1.LT.N*H/N9) N1=N	368
420 CONTINUE	359
DO 430 N=1,N9	370
RRR1=R1+(N-1)*WID1/N9	371
RRF2=R1+N*WIC1/N9	372
IF(R.GE.RRR1.AND.R.LT.RRF2) N2=N	373
430 CONTINUE	374
AMAT(N1,N2)=AMAT(N1,N2)+1.0	375
C DO WE HIT THE CHANNELTRON?	376
RR=(R1+R2B)/2.0	377
C FULL DEFORESTESA CARDS	378
DIS2=AL3	379
DT=DIS2/VTT	380
XX=0.0	381
XX=VTT	382
VT=VOLT1	383
DTT=0.1*DT	384
TT=0.0	385
ACC=QC*MP*VT/DIS2	386
460 CONTINUE	387
TT=TT+DTT	388
XX=XX+VXX*DTT-ACC*DTT**2/2.0	389
VXX=VXX-ACC*DTT	390
C DOES LOW-ENERGY ELECTRON STOP	391
IF(VXX.LE.0.0) GO TO 202	392

BEST AVAILABLE COPY

```

IF(XX,LT,DIS2) GO TO 460          393
R=F+VP*TT                         394
Z1=Z1+VZ*TT                         395
IF(IJ.NE.0) R5=1.77E-03             396
IF(IJ.NE.0) R9=-R5                 397
R4=ABS(RR-R9-R)                   398
C PULL OUT CEFOREST CARDS        399
  IF(R.LT.(RR-A2/2.0).OR.R.GT.(RR+A2/2.0)) GO TO 202 400
  IF(Z1.GT.B2.OR.Z1.LT.0.0) GO TO 202 401
  R4A=SQRT(R4**2+(Z1-B2/2.0-R5)**2) 402
  R4B=SQRT(R4**2+(Z1-B2/2.0+R5)**2) 403
  IF(R4A.GT.R5.AND.R4B.GT.R5) GO TO 202 404
    IF(IK.GE.2) AX(K13)=AX(K13)+1.0 405
  COUNT=COUNT+1                     406
  GO TO 202                         407
500 CONTINUE                         408
EFF(K)=COUNT/CNT                  409
  IF(IK.GE.2) AX(K13)=AX(K13)/CNT 410
EG(K)=EE(K)/1.6E-19                411
  CNTA=CNNTA+CNTA                 412
  PFINT 507,EG(K),CNTA,CNNTA      413
507 FORMAT(1X,* AT ENERGY = *,1PE10.2,* EV NUMBER OF PA 414
+RTICLES                           414
1 THROUGH APERTURE= *,0FF10.2, * RUNNING TOTAL= *,0FF10.2) 415
  IF(IJ.EQ.1) GO TO 630             416
    E99=EG(K)/1.0E 03               417
    EFI=1.0                          418
    TEMP=EG(K)                      419
    EG(K)=EG(K)-VT+POST             420
    IF(PART.EQ.ELEC.AND.EG(K).GE.1.0E 03.AND.EG(K).LE.5.0E 0 421
+6)                                421
    1 EFI=1.0-(2.0/(3.0+6.5/(E99 -0.5)+30./*(E99 -0.5)**3)) 422
    IF(PART.EQ.ELEC.AND.EG(K).GE.10.0.AND.EG(K).LE.70.) EFI=0 423
    +.10*EG(K)                      423
    1**0.515                         424
    IF(PART.EQ.ELEC.AND.EG(K).GE.200.AND.IJ.NE.0) EFI=8.199/EG 425
    +(K)**0.41                        425
A7
  IF(PART.EQ.ELEC.AND.EG(K).LT.200.AND.IJ.NE.0) EFI=5.9E-04* 426
  +EG(K)**1.                          427
A38
  EG(K)=TEMP                         428
    IF(IK.GE.2) AX(K13)=AX(K13)*EFI 429
    IF(IK.GE.2) GO TO 440             430
  EFF(K)=EFF(K)*EFI                 431
  IF(IJ.EQ.2) EFF(K)=EFF(K)*2.0E 06 432
    IF(MCD(K,N7).NE.0) GO TO 440     433
    E1=EE(K-N7+1)/1.6E-19            434
    E2=EE(K)/1.6E-19                 435
    AN7=N7                            436
    DO 435 N=1,N9                    437
                                         438

```

BEST AVAILABLE COPY

```

SUM1(N)=0.0          439
DO 435 I=1,N9        440
SUM1(N)=SUM1(N)+AMAT(I,N) 441
435 CONTINUE         442
    AN8=N7*TOT        443
    PRINT 433,E1,E2,((AMAT(N1,N2),N2=1,N9),N1=1,N9),(SUM1(N),
+N=1,N9), 444
    1AN8              445
433 FORMAT(1X,*EFFICIENCY MATRIX FOR EXIT APERTURE OF ESA FLA 446
+TES FRCM           446
1ENERGY=*,1PE10.2,*EV*,*TO*,1PE10.2,*EV*/0P5F10.2/5F10.2/5 447
+F10.2/5F1 447
Z0.2/5F10.2/1X,*TOTALS*/5F10.2,*PARTICLES TRACED=*,1PE10.2 448
+//)               448
    DO 438 I=1,10      449
    DO 438 N=1,10      450
    AMAT(I,N)=0.0       451
438 CONTINUE          452
440 CONTINUE          453
    IF(IK.GE.2) K13=K13+1 454
    IF(IK.GE.2.AND.K13.LT.N11) GO TO 37 455
    IF(IK.GE.2) GO TO 610 456
    GO TO 600            457
600 CONTINUE          458
    CALL SIMP           459
610 CONTINUE          460
    IF(IK.EQ.3) PPRINT 613 461
613 FORMAT(1X,*ANGULAR SCAN IN Z-PLANE*) 462
    IF(IK.EQ.2) PRINT 609 463
609 FCMPMAT(1X,*ANGULAR SCAN IN R-PLANE*) 464
    IF(IK.GE.2) PRINT 611, (THM(K),AX(K),K=1,N11) 465
511 FORMAT((1P12E10.2)) 466
    IF(IK.GE.2) GO TO 24 467
630 CONTINUE          468
    THR=THW*AA          469
    IF(IJ.EQ.2) PRINT 740,THR 470
740 FORMAT(1X,*ELECTRONS FROM GUN INCIDENT ON APERTURE AT AN 471
+ANGLE CF           471
740 A *,F7.2,* DEG*) 472
    PRINT 51             473
51  FORMAT(1X,*EFFICIENCY OF CHANNELTRON TO SEE PARTICLES*) 474
    PRINT 55,(EG(K),EFF(K),K=1,N5) 475
55  FORMAT(1X,*ENERGY-EFFICIENCY*/(1P10E12.2)) 476
    G1=G*GINT           477
    PRINT 63,GINT,G1     478
63  FORMAT(1X,*INTEGRAL OF CHANN. EFFIC.=*,1PE10.4,* EV*,3X,* 479
+NORMALIZA          479
    ITION FACTOR FOR ENTIRE ESA=*,1PE10.4,* CMSQ-SR-EV*) 480
    HH=G1/EA            481
    PRINT 67,HH          482
67  FORMAT(1X,*DEFOREST H-FACTOR=*,1PE10.4,* CMSQ-SR*) 483
    GO TO 1              484
    END                  485

```

BEST AVAILABLE COPY

SUBROUTINE SIMP	466
DIMENSION EFF(200),EG(200)	487
COMMON/F1/EFF,EG,DELE,N5,GINT	488
C SIMPSON RULE	489
DEL=DELE/1.6E-19	490
N6=N5-3	491
N7=N5-2	492
SUM1=0.0	493
DO 10 J=3,N6,2	494
SUM1=SUM1+EFF(J)	495
10 CONTINUE	496
SUM2=0.0	497
DO 20 J=2,N7,2	498
SUM2=SUM2+EFF(J)	499
20 CONTINUE	500
GINT=(EFF(1)+EFF(N5-1)+4.0*SUM2+2.0*SUM1)*DEL/3.0	501
RETURN	502
END	503

BEST AVAILABLE COPY

REFERENCES

Pantazis, John; Huber, Alan; and Hagan M.P., Design of Electrostatic Analyzer, AFGL-TR-77-0120, 1977.

Archuleta, R.J. and DeForest, J.E., Efficiency of Channel Electron Multipliers for Electrons of 1-50 keV, Rev. of Sci. Instru., 42, 89-91, 1971.

Willis, D.M. and Thomas, G.R., Geometric Factor of a Cosmic Ray Detector: Equivalence of Alternative Analytical Derivations, Eldo-Cecles/ESRO-Cess Scient. and Tech. Rev., 4, 101-102, 1972.

Sullivan, J.D., Geometrical factor and directional response of single and multi-element particle telescopes, Instr. and Methods, 95, 5-11, 1971.

Rothwell, Paul L., and Moomey, Wayne R., Calibration of a Magnetic Spectrometer Designed to Measure 0.1 -1.0 MeV Electrons in Space, AFCRL-72-0710, 1972.

